applied biosciences

MDPI

Article

Anti-Obesity Effects of *Artocarpus integer* Stem Bark Extract via Appetite and Lipid Metabolism Modulation in Obese Rats

Anton Bahtiar [1,*], Sekar Ayu Rabbani [1], Asfareni Rahmah [1] and Sirithon Siriamornpun [2]

[1] Disease-Related Biomarker and Prospective Therapy Cluster, Faculty of Pharmacy, Universitas Indonesia, Kampus UI Depok, Depok 16424, West Java, Indonesia; asfaraeni.rahmah@ui.ac.id (A.R.)
[2] Research Unit of Thai Food Innovation, Department of Food Technology, Faculty of Technology, Mahasarakham University, Mahasarakham 44150, Thailand; sirithon.s@msu.ac.th
* Correspondence: anton.bahtiar@farmasi.ui.ac.id

Abstract

Obesity is a multifactorial metabolic disorder characterized by dysregulated energy homeostasis, impaired lipid metabolism, and altered hypothalamic appetite signaling. This study aimed to evaluate the anti-obesity effects and underlying mechanisms of a 95% ethanol extract of *Artocarpus integer* stem bark in a high-fat diet (HFD)-induced obese rat model. Obesity was induced in male Wistar rats using HFD feeding, followed by treatment with the extract (200–800 mg/kg/day, oral). Semaglutide and resveratrol were used as reference compounds. Body weight, food intake, adiposity, serum lipid profile, adipokines, histological changes, and gene expression related to lipid metabolism (Fas, Pparγ, Cpt-1, AdipoR1) and hypothalamic appetite regulation (Pomc, Mc4r, Npy) were evaluated. Phytochemical profiling was performed using LC–HRMS. The extract markedly reduced body weight gain, visceral adiposity, and food intake compared with the HFD control ($p < 0.05$), with the high-dose extract demonstrating a substantial weight-reducing effect that approached the magnitude of semaglutide. Treatment improved dyslipidemia by decreasing total cholesterol and triglycerides while increasing HDL levels. Adipokine imbalance was restored, as evidenced by reduced leptin and amylin and increased adiponectin levels. At the molecular level, the extract downregulated lipogenic genes (Fas, Pparγ), partially restored Cpt-1 expression, and normalized AdipoR1. In the hypothalamus, Pomc and Mc4r were upregulated, whereas Npy was suppressed. LC–HRMS analysis revealed the presence of stilbene, chalcone, and flavonoid derivatives. In conclusion, *A. integer* stem bark extract exerts anti-obesity effects through coordinated modulation of appetite signaling and lipid metabolism, supporting its potential as a multi-target phytotherapeutic agent for obesity management.

Keywords: *Artocarpus integer*; obesity; appetite regulation; lipid metabolism; LC–HRMS

Check for updates

Academic Editors: Cristiane Aguiar Da Costa and Graziele Freitas De Bem

Received: 23 July 2026
Revised: 29 August 2026
Accepted: 7 September 2026
Published: 8 September 2026

Copyright: © 2026 by the authors. Licensee MDPI, Basel, Switzerland. This article is an open access article distributed under the terms and conditions of the Creative Commons Attribution (CC BY) license.

1. Introduction

Obesity is a complex and multifactorial metabolic disorder characterized by excessive adipose tissue accumulation resulting from a chronic imbalance between energy intake and expenditure. Beyond increased fat mass, obesity is associated with profound metabolic dysregulation, including altered adipokine secretion, impaired lipid metabolism, and disruption of central appetite-regulating pathways [1]. These abnormalities contribute to the development of major comorbidities such as type 2 diabetes mellitus, cardiovascular disease, and stroke, highlighting the urgent need for effective and safe therapeutic interventions [2].

Current pharmacological strategies for obesity management remain limited in long-term efficacy [3]. Conventional anti-obesity agents typically produce modest weight reduction, whereas glucagon-like peptide-1 receptor agonists (GLP-1 RAs), such as semaglutide, have demonstrated improved clinical outcomes [4]. The therapeutic effects of GLP-1 RAs are primarily mediated through modulation of hypothalamic signaling, including activation of proopiomelanocortin (*Pomc*) neurons and suppression of neuropeptide Y (*Npy*)-driven orexigenic pathways [5]. Despite their efficacy, these agents are associated with high cost, limited accessibility, and potential adverse effects, underscoring the need for alternative or complementary pharmacological approaches, particularly those with multi-target mechanisms.

Natural products have emerged as promising sources of bioactive compounds with the ability to modulate multiple metabolic pathways involved in obesity. Several phytochemicals, including berberine, curcumin, quercetin, and resveratrol, have demonstrated anti-obesity activity through coordinated regulation of adipogenesis, enhancement of fatty acid oxidation, and modulation of appetite-related signaling [6]. Among these, resveratrol, a stilbene-derived polyphenol, has been shown to activate mitochondrial fatty acid oxidation and suppress adipogenic gene expression [7]. However, its overall efficacy in reducing body weight remains limited, suggesting that structurally related compounds or complex phytochemical mixtures may provide enhanced pharmacological activity through synergistic multi-target effects.

Stilbenes are phytoalexins synthesized via the phenylpropanoid pathway and are widely distributed in species of the genus *Artocarpus* (Moraceae), particularly in stem bark tissues [8]. *Artocarpus integer* (Thunb.) Merr., commonly known as cempedak, is a rich source of stilbene derivatives, chalcones, and flavonoids, which have been associated with anti-adipogenic, lipid-modulating, and appetite-regulating activities [9]. Although related species, such as *Artocarpus heterophyllus*, have demonstrated inhibitory effects on adiposity [10], the pharmacological potential and molecular mechanisms of *A. integer* stem bark in obesity remain insufficiently characterized. Recent evidence demonstrates that stilbenoids suppress adipogenesis and lipogenesis by activating AMP-activated protein kinase (AMPK) and downregulating key adipogenic transcription factors (PPAR-γ and C/EBPα), while promoting lipid turnover and thermogenesis [11].

In this context, the present study aimed to evaluate the anti-obesity effects and underlying pharmacological mechanisms of a 95% ethanol extract of *A. integer* stem bark in a high-fat diet-induced obese rat model. The extract was assessed in comparison with semaglutide and resveratrol as reference compounds. Both central and peripheral mechanisms were investigated through analysis of body weight, adiposity, lipid profile, adipokine levels, histological alterations, and gene expression associated with lipid metabolism (*Cpt-1*, *Fas*, *Pparγ*, and *AdipoR1*) and hypothalamic appetite regulation (*Pomc*, *Mc4r*, and *Npy*) [12]. This integrated approach was designed to elucidate the potential of *A. integer* as a multi-target phytotherapeutic agent for obesity management.

2. Materials and Methods

2.1. Study Design

This study was conducted using a randomized controlled experimental design to evaluate the pharmacological effects of *Artocarpus integer* (Thunb.) Merr. stem bark extract in a high-fat diet (HFD)-induced obese rat model. The experimental protocol was structured to assess both efficacy and mechanistic outcomes, including body weight, adiposity, food intake, serum metabolic parameters, adipokine profiles, histological alterations, and gene expression associated with lipid metabolism and hypothalamic appetite regulation.

Obesity was first established through HFD feeding, and animals meeting predefined obesity criteria were subsequently randomized into treatment groups. The extract was administered at multiple dose levels to evaluate dose–response relationships, with semaglutide and resveratrol included as pharmacological reference compounds. This design enabled comparative evaluation of the extract's anti-obesity efficacy and its effects on central (hypothalamic signaling) and peripheral (lipid metabolism) regulatory pathways [12].

2.2. Experimental Animals

Male Wistar rats (7–8 weeks old; 120–140 g) were used in this study. Animals were acclimatized for 14 days under controlled laboratory conditions (temperature 22 ± 2 °C, relative humidity 55 ± 10%, and a 12 h light/dark cycle) with ad libitum access to standard chow and water. Male animals were selected to minimize variability associated with hormonal fluctuations and to ensure consistency in metabolic responses to high-fat diet (HFD) induction. However, the use of a single sex represents a limitation for the generalizability of the findings, and future studies should include both sexes to evaluate potential sex-specific differences in the anti-obesity effects of *Artocarpus integer* extract.

Diet-induced obesity was established by feeding animals a high-fat diet (HFD) consisting of standard chow (50%), beef tallow (20%), sucrose (20%), and butter (10%) [13,14]. The HFD was administered until animals met predefined obesity criteria, including a Lee index > 315, body mass index (BMI) > 0.68, and at least a 50% increase in body weight relative to baseline. These parameters were used to confirm successful induction of obesity before initiation of treatment.

2.3. Plant Material and Extraction

The stem bark of *Artocarpus integer* (Thunb.) Merr. (Moraceae) was obtained from the Indonesian Research Institute for Spices and Medicinal Plants (Balittro, Bogor, Indonesia) and authenticated by the Indonesian National Research and Innovation Agency (BRIN). A voucher specimen (No. B-86/II.6.2/IR.01.02/1/2025) was deposited at Herbarium Bogoriense, Directorate of Scientific Collection Management, BRIN (Cibinong, Indonesia), for future reference.

Dried plant material (5.0 kg) was powdered and extracted with 95% ethanol by maceration (three consecutive cycles of 24 h at room temperature). The combined extracts were filtered and concentrated under reduced pressure to obtain a crude extract. The extraction yielded 265.9 g of crude extract, corresponding to a yield of 5.31% (*w*/*w*) and a drug–extract ratio (DER) of 18.8:1.

Phytochemical profiling was performed using liquid chromatography–high-resolution mass spectrometry (LC–HRMS). Chromatographic separation was carried out on an Accucore™ Phenyl Hexyl column (100 × 2.1 mm, 2.6 µm) maintained at 40 °C. The mobile phase consisted of 0.1% formic acid in water (solvent A) and 0.1% formic acid in acetonitrile (solvent B), delivered at a flow rate of 0.3 mL/min using a gradient elution from 5% to 90% B over 16 min.

2.4. Experimental Groups and Treatment Protocol

Following confirmation of diet-induced obesity, animals were randomly assigned to experimental groups using a random allocation method to minimize selection bias. The animals were allocated into seven groups (n = 6 per group): (1) normal control (standard diet + vehicle), (2) HFD control (high-fat diet + vehicle), (3) semaglutide-treated group (70 µg/kg body weight, intramuscular), (4) resveratrol-treated group (30 mg/kg body weight/day, oral), (5) *A. integer* extract low dose (200 mg/kg body weight/day, oral), (6) *A. integer* extract medium dose (400 mg/kg body weight/day, oral), and (7) *A. integer* extract high dose (800 mg/kg body weight/day, oral).

The selected extract doses were based on previous pharmacological studies of *Artocarpus* species demonstrating metabolic regulatory activity [15]. Semaglutide and resveratrol were included as reference compounds due to their established anti-obesity and metabolic effects, enabling comparative evaluation of efficacy.

The vehicle consisted of sodium phosphate dibasic (44 mM), sodium chloride (70 mM), and Tween 20 (0.007%) [16]. Oral treatments were administered by gavage at a volume of 1 mL/100 g body weight, while semaglutide was administered intramuscularly at 1 mL/kg body weight. All treatments were administered throughout the experimental period under consistent conditions.

2.5. Measurement of Obesity and Metabolic Parameters

Body weight and food intake were recorded daily throughout the experimental period to evaluate changes in energy balance. Body mass index (BMI) and Lee index were calculated weekly using body weight and naso–anal length to monitor the progression of obesity.

At the end of the treatment period, blood samples were collected and centrifuged to obtain plasma for biochemical analysis. Plasma concentrations of leptin, amylin (islet amyloid polypeptide, IAPP), and adiponectin were quantified using commercially available enzyme-linked immunosorbent assay (ELISA) kits (Fine Test, Wuhan, China; leptin: ER0115; amylin/IAPP: ER0374; adiponectin: ER0006), according to the manufacturers' protocols.

Semaglutide (CAS: 910463-68-2) was obtained from Cayman Chemical (Ann Arbor, MI, USA; Cat. No. 40231), and Resveratrol (≥99% purity) was purchased from Macklin (Shanghai, China; Cat. No. R817263).

2.6. Gene Expression Analysis

At the end of the treatment period, animals were anesthetized with a ketamine–xylazine combination and euthanized. The hypothalamus was rapidly dissected, snap-frozen in liquid nitrogen, and stored at −80 °C until analysis.

Total RNA was extracted using TRIzol reagent, followed by DNase I treatment to remove genomic DNA contamination. Complementary DNA (cDNA) was synthesized using reverse transcriptase according to the manufacturer's instructions. Quantitative real-time polymerase chain reaction (RT–qPCR) was performed using SYBR Green chemistry on a CFX96 Real-Time PCR Detection System (Bio-Rad, Hercules, CA, USA).

Gene expression analysis was conducted for markers involved in lipid metabolism (*Fas*, *Cpt-1*, *Pparγ*, and *AdipoR1*) and hypothalamic appetite regulation (*Pomc*, *Mc4r*, and *Npy*). β-Actin was used as the internal reference gene [12,17]. Primer sequences were ordered and designed by PT Indogen (Jakarta, Indonesia) and synthesized commercially (PCR grade) and are listed in Table 1. All gene expression analyses were performed by investigators blinded to group allocation to ensure unbiased data acquisition and interpretation.

Table 1. Primer sequences used for RT–qPCR analysis.

Gene	Direction	Sequence (5′–3′)
Fas	Forward	AGC CTA ACT CCT CGC TGC AAT
Fas	Reverse	TCC TTG GAA CCG TCT GTG TTC
Cpt-1	Forward	AGG GCC ACT GAT GGT GAA C
Cpt-1	Reverse	TGC CTG AAT CGA AGT GGG T
Pomc	Forward	CCT GTG AAG GTG TAC CCC AAT GTC
Pomc	Reverse	CAC GTT CTT GAT GAT GGC GTT C
Npy	Forward	CCC GCC CGC CAT GAT GCT AGG
Npy	Reverse	CCG CCC GGA TTG TCC GGC TTG

Table 1. *Cont.*

Gene	Direction	Sequence (5′–3′)
Mc4r	Forward	AAC ATT CTA GTG ATC GTG GG
Mc4r	Reverse	CAT AAT GTT ATG GTA CTG GAG CGC G
β-actin	Forward	TGA CGT GGA CAT CCG CAA AG
β-actin	Reverse	CTG GAA GGT GGA CAG CGA GG

The RNA purity metrics (A260/A280 ratio of 1.95–2.05), cDNA input concentrations, thermal cycling conditions, and melt curve analysis confirm single-product specificity.

2.7. Histological Analysis of Adipose Tissue

At the end of the experimental period, animals were anesthetized and euthanized as described above. Peripheral adipose tissue was excised, rinsed with physiological saline to remove residual blood, and fixed in 10% neutral buffered formalin for at least 24 h.

Fixed tissues were processed using standard histological procedures, including dehydration through a graded ethanol series, clearing in xylene, and embedding in paraffin. Tissue sections (4–5 μm) were prepared using a microtome, mounted on glass slides, deparaffinized, rehydrated, and stained with hematoxylin and eosin (H&E) [18].

Histological evaluation was performed using a light microscope (Olympus, Tokyo, Japan). Representative images were captured digitally, and morphometric analysis of adipocytes was conducted using ImageJ (National Institutes of Health, Maryland, DC, USA). Adipocyte diameter and circumference were measured from at least 50 randomly selected cells per sample, and mean values were calculated for each animal. Investigators performing histological and morphometric analyses were blinded to group allocation to minimize observer bias.

2.8. Statistical Analysis

Data are expressed as mean ± standard deviation (SD). Statistical analyses were performed using SPSS version 22 (IBM Corp., New York, NY, USA, licensed software). Data distribution was assessed using the Shapiro–Wilk test, and homogeneity of variance was evaluated using Levene's test.

For normally distributed data with homogeneous variances, comparisons among multiple groups were performed using one-way analysis of variance (ANOVA) followed by Bonferroni's post hoc test. When the assumption of homogeneity of variance was violated, Welch's ANOVA followed by the Games–Howell post hoc test was applied. Non-normally distributed data were analyzed using the Kruskal–Wallis test followed by Dunn's post hoc test.

For comparisons between two groups, the independent samples *t*-test was used for parametric data, while the Mann–Whitney U test was applied for nonparametric data. A p-value < 0.05 was considered statistically significant.

3. Results

3.1. LC-HRMS Profiling of A. integer Stem Bark Extract

The LC–HRMS total ion chromatogram (TIC) of the 95% ethanol extract of *Artocarpus integer* stem bark (Figure 1) revealed a chemically complex profile with multiple well-resolved peaks across the retention time range, indicating the presence of diverse secondary metabolites. The distribution of peaks suggested a predominance of moderately polar to semipolar compounds, consistent with the extraction solvent used.

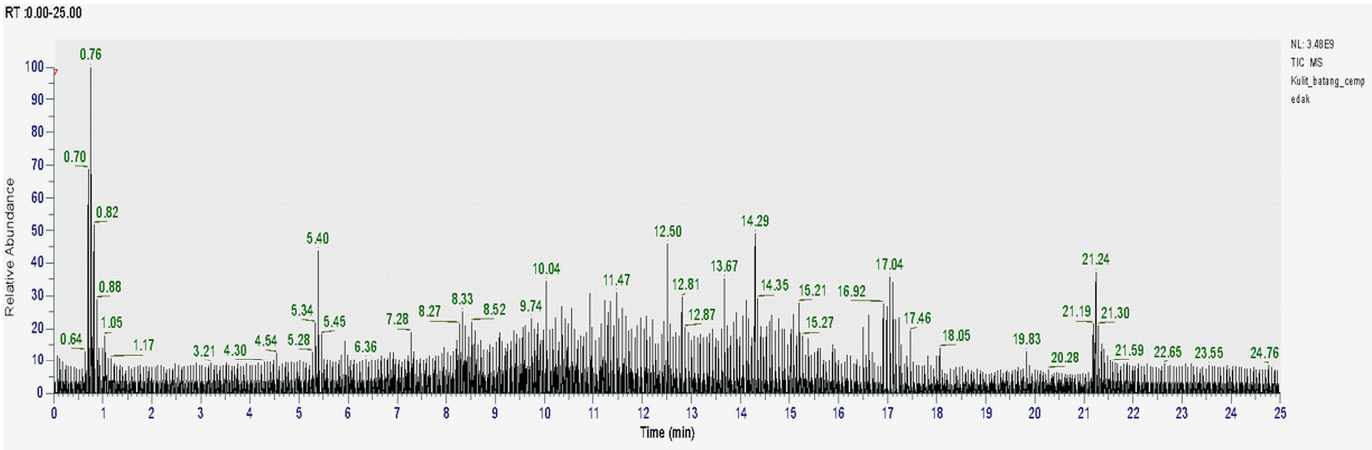


Figure 1. LC–HRMS Total Ion Chromatogram of *A. integer* Stem Bark Extract.

Tentative compound identification (Table 2) indicated the presence of several bioactive classes, including stilbenes, chalcones, and flavonoids. These phytochemicals are widely associated with metabolic regulatory effects, particularly through modulation of lipid metabolism and adipogenesis. For instance, stilbene derivatives are linked to activation of fatty acid oxidation pathways, while chalcones and flavonoids have been reported to suppress lipogenic signaling and adipocyte differentiation.

Table 2. Major phytochemical constituents of *A. integer* stem bark extract and their reported bioactivities.

Compound	Class	Reported Bioactivity
Stilbene (cis-/trans-)	Stilbene	Anti-adipogenic; modulates lipid metabolism
Resveratrol (cis/trans)	Stilbene	Activates fatty acid oxidation; suppresses lipogenesis
Cycloartocarpin	Prenylated flavonoid	Inhibits adipogenesis; anti-inflammatory
Roburic acid	Triterpenoid	Anti-inflammatory; modulates lipid metabolism
Methoxylated chalcone	Chalcone	Suppresses adipogenesis; activates AMPK
Bakuchalcone	Chalcone	Reduces lipid accumulation; antioxidant
Glabrachalcone	Chalcone	Inhibits adipocyte differentiation
Isogemichalcone B	Chalcone	Suppresses lipogenic gene expression
Lumaflavanone C	Flavonoid	Improves lipid profile; antioxidant
Macrophyllol A	Flavonoid	Modulates lipid metabolism

Notes: Compound identification was tentative and based on accurate mass measurements and comparison with spectral databases and published literature. RT, retention time; m/z, mass-to-charge ratio; AMPK, AMP-activated protein kinase; SIRT1, sirtuin 1; CPT-1, carnitine palmitoyltransferase-1; PPARγ, peroxisome proliferator-activated receptor gamma; FAS, fatty acid synthase.

The coexistence of these compound classes suggests a potential synergistic, multi-target mode of action underlying the observed anti-obesity effects of the extract. However, it should be noted that compound identification was based on accurate mass analysis and literature comparison; therefore, further confirmation using tandem mass spectrometry (MS/MS) and authentic standards is required.

Total ion chromatogram (TIC) of the 95% ethanol extract of *A. integer* stem bark obtained using LC–HRMS. Chromatographic separation was performed on an Accucore™ Phenyl Hexyl column with gradient elution of 0.1% formic acid in water (A) and acetonitrile (B) at a flow rate of 0.3 mL/min.

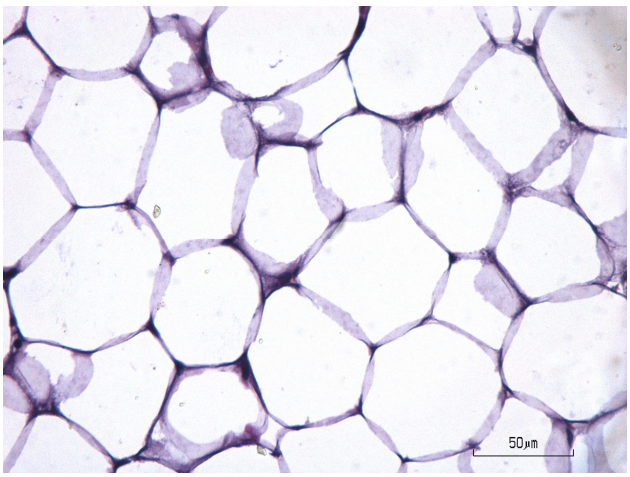
Comprehensive LC–HRMS profiling data, including retention times (RT), mass-to-charge ratios (m/z $[M+H]^+$), tentative compound identifications, and detailed annotations, are provided in Supplementary Table S1.

3.2. Effects of *A. integer* Extract on Body Weight Gain

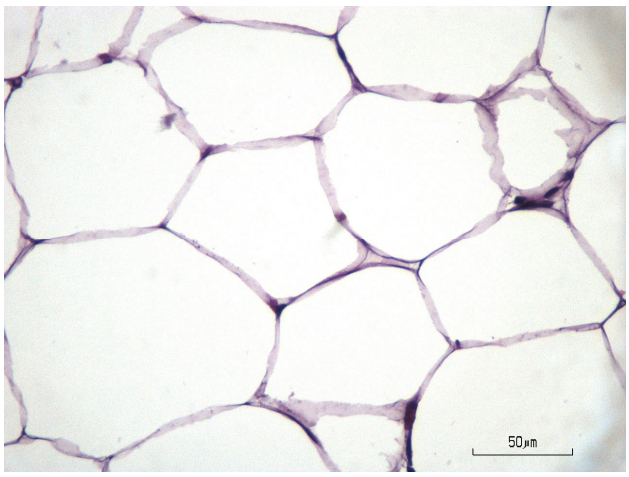
Body weight changes over the 15-week experimental period are shown in Figure 2. During the pre-induction phase (weeks 1–4), no significant differences in body weight were observed among groups ($p > 0.05$), indicating comparable baseline conditions. High-fat diet (HFD) feeding (weeks 5–10) resulted in a significant increase in body weight in the HFD group compared with the normal control ($p < 0.05$), confirming successful induction of obesity.

During the treatment phase (weeks 11–15), the HFD control group exhibited a continued progressive increase in body weight. In contrast, semaglutide significantly attenuated body weight gain ($p < 0.05$ vs. HFD), while resveratrol produced a moderate effect. Administration of *A. integer* extract resulted in a dose-dependent reduction in body weight gain. The highest dose (800 mg/kg) significantly decreased body weight compared with the HFD group ($p < 0.05$), with efficacy comparable to semaglutide. The intermediate (400 mg/kg) and low (200 mg/kg) doses also significantly reduced body weight gain, although to a lesser extent.

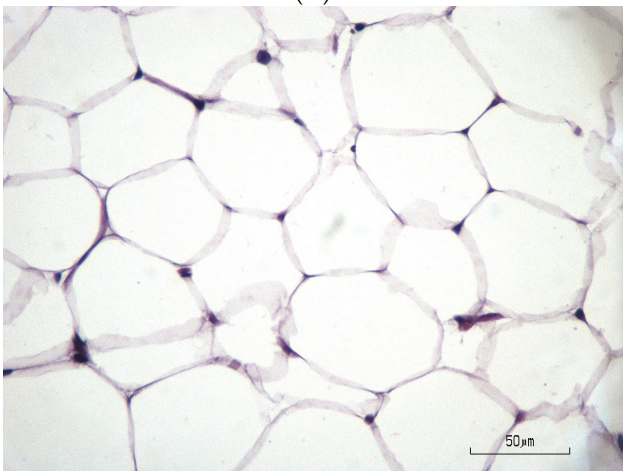
These findings demonstrate that *A. integer* extract effectively attenuates HFD-induced body weight gain in a dose-dependent manner, supporting its anti-obesity efficacy. Interestingly, the magnitude of weight reduction observed with the highest extract dose approached that of semaglutide, showing a marked reduction in body weight gain relative to the HFD control, approaching the magnitude of reduction seen in the semaglutide group with values comparable to those observed in the semaglutide-treated group.



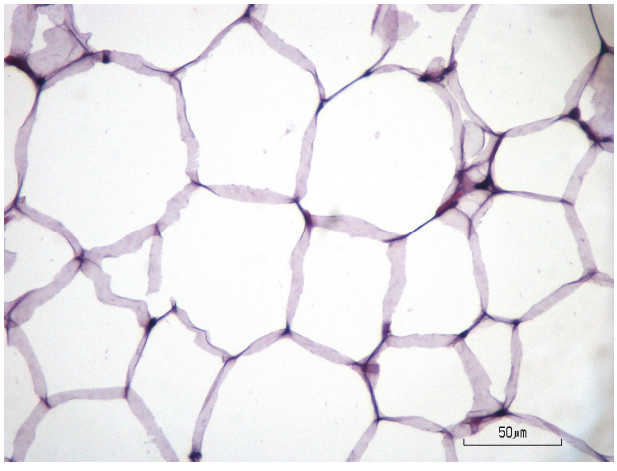
(**A**)



(**B**)

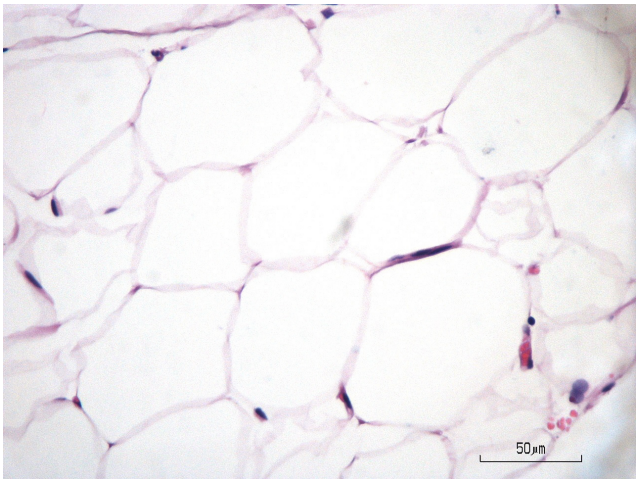


(**C**)

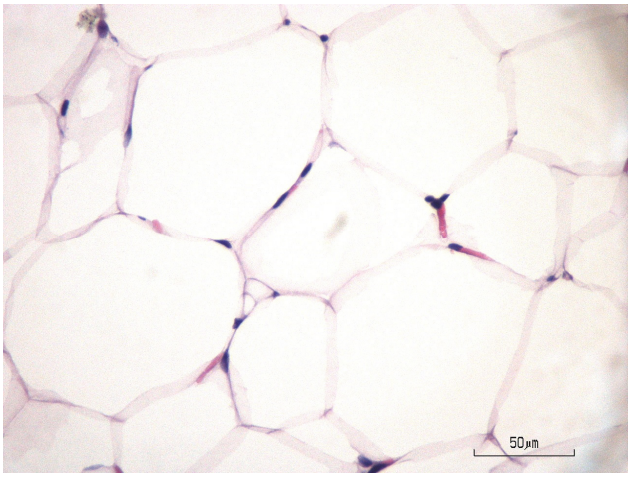


(**D**)

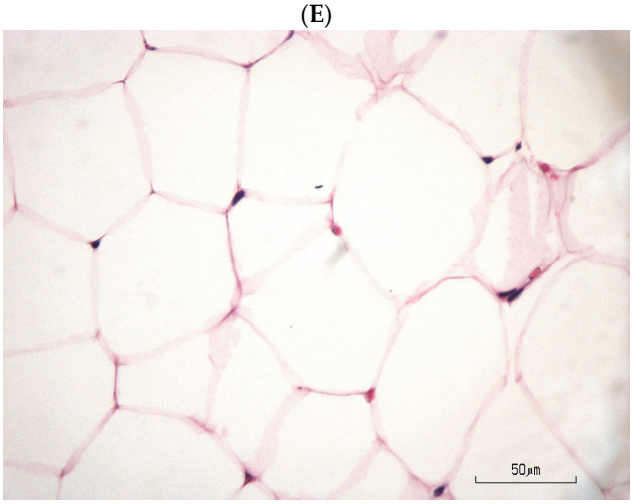
Figure 2. *Cont.*



(**E**)



(**F**)



(**G**)

Figure 2. Effects of *A. integer* Stem Bark Extract on Body Weight Gain in HFD-Induced Obese Rats. Changes in body weight over the 15-week experimental period. Data are presented as mean ± standard deviation (SD) ($n = 6$). Normal, standard diet + vehicle; HFD, high-fat diet + vehicle; semaglutide (70 μg/kg, intramuscular); resveratrol (30 mg/kg/day, oral); AIE-L (200 mg/kg/day, oral); AIE-M (400 mg/kg/day, oral); AIE-H (800 mg/kg/day, oral). $p < 0.05$ versus the HFD control group. Histopathological Changes in Adipose Tissue of HFD-Induced Obese Rats. Representative hematoxylin–eosin (H&E)-stained sections of adipose tissue (scale bar = 50 μm). (**A**) Normal; (**B**) HFD; (**C**) semaglutide (70 μg/kg); (**D**) resveratrol (30 mg/kg); (**E**) AIE-L (200 mg/kg); (**F**) AIE-M (400 mg/kg); (**G**) AIE-H (800 mg/kg).

3.3. Effects of A. integer Extract on Epididymal Adipose Tissue Weight and Adiposity Index

The effects of *A. integer* stem bark extract on epididymal adipose tissue weight and adiposity index are summarized in Table 3. High-fat diet (HFD) feeding significantly increased both parameters compared with the normal control group ($p < 0.05$), confirming the development of visceral adiposity.

Treatment with semaglutide significantly reduced epididymal adipose tissue weight and adiposity index compared with the HFD control ($p < 0.05$), whereas resveratrol produced a moderate reduction. Administration of *A. integer* extract resulted in a dose-dependent attenuation of visceral adiposity. The highest dose (800 mg/kg) markedly reduced both adipose tissue weight and adiposity index ($p < 0.05$ vs. HFD), reaching levels numerically close to those observed in the semaglutide-treated cohort. The intermediate dose (400 mg/kg) also produced significant reductions, while the lowest dose (200 mg/kg) showed moderate but significant effects.

Table 3. Effects of *A. integer* stem bark extract on epididymal adipose tissue weight and adiposity index.

Parameter	Normal	HFD	Semaglutide	Resveratrol	AIE-L	AIE-M	AIE-H
Epididymal adipose tissue weight (g)	4.87 ± 1.3	19.27 ± 3.4 [a]	6.28 ± 3.0 [b]	9.72 ± 3.0 [ab]	9.49 ± 1.4 [ab]	8.4 ± 2.2 [b]	6.17 ± 1.9 [b]
Adiposity index (%)	2.45 ± 0.7	6.43 ± 1.8 [a]	2.83 ± 1.3 [b]	4.55 ± 1.6 [a]	4.54 ± 0.7 [a]	3.96 ± 1.7	2.82 ± 0.9 [b]

Notes: Data are presented as mean ± standard deviation (SD) ($n = 6$). Normal, standard diet + vehicle; HFD, high-fat diet + vehicle; semaglutide (70 μg/kg, intramuscular); resveratrol (30 mg/kg/day, oral); AIE-L (200 mg/kg/day, oral); AIE-M (400 mg/kg/day, oral); AIE-H (800 mg/kg/day, oral). [a] $p < 0.05$ vs. normal control group; [b] $p < 0.05$ vs. HFD control group.

These results indicate that *A. integer* extract effectively reduces HFD-induced visceral fat accumulation in a dose-dependent manner, supporting its anti-adipogenic and lipid-modulating activity.

3.4. Effects of A. integer Extract on Food Intake and Appetite-Related Hormones

The effects of *A. integer* stem bark extract on food intake and appetite-related hormones are summarized in Table 4. High-fat diet (HFD) feeding resulted in increased food intake and significant alterations in circulating adipokines compared with the normal control group ($p < 0.05$), indicating dysregulation of energy balance and metabolic homeostasis.

Table 4. Effects of *A. integer* extract on food intake and adipokines (% change vs. HFD).

Parameter	Semaglutide	Resveratrol	AIE-L	AIE-M	AIE-H
Food intake	−44%	−14%	−18%	−21%	−37%
Leptin	−47%	−35%	−36%	−45%	−52%
Amylin	−45%	−30%	−31%	−39%	−47%
Adiponectin	+261%	+143%	+146%	+208%	+267%

Notes: Values in the main text table represent percentage changes relative to the HFD control group. Absolute mean ± SD values for daily food intake (g/day) and plasma concentrations of leptin (pg/mL), amylin (pg/mL), and adiponectin (μg/mL) across all individual experimental groups are reported in Supplementary Table S2.

During the treatment phase, semaglutide significantly reduced food intake compared with the HFD control ($p < 0.05$), whereas resveratrol exerted a modest effect. Administration of *A. integer* extract led to a dose-dependent reduction in food intake. The highest dose (800 mg/kg) significantly decreased food intake ($p < 0.05$ vs. HFD), with efficacy comparable to semaglutide, while the intermediate (400 mg/kg) and low (200 mg/kg) doses produced moderate reductions.

Relative percentage modifications in daily food consumption and circulating adipokine concentrations compared to the HFD control group are summarized in Table 4. Complete absolute raw values (mean ± SD) for post-treatment daily food intake (e.g., 10.4 ± 3.1 g/day in AIE-H vs. 16.4 ± 2.7 g/day in HFD) as well as plasma concentrations of leptin (pg/mL), amylin (pg/mL), and adiponectin (μg/mL) across all seven experimental cohorts are provided in Supplementary Table S2.

HFD feeding markedly increased plasma leptin and amylin levels and reduced adiponectin concentrations ($p < 0.05$ vs. normal), reflecting obesity-associated hormonal imbalance. Treatment with *A. integer* extract significantly reversed these alterations in a dose-dependent manner. The highest dose (800 mg/kg) reduced leptin and amylin levels and restored adiponectin concentrations to near-normal levels ($p < 0.05$ vs. HFD), with effects comparable to semaglutide. Lower doses also improved adipokine profiles, although to a lesser extent.

This pattern suggests not only improved metabolic status but also partial restoration of adipose tissue endocrine function.

3.5. Effects of A. integer Extract on Serum Lipid Profile

The effects of *A. integer* stem bark extract on serum lipid parameters are presented in Table 5. High-fat diet (HFD) feeding induced pronounced dyslipidemia, characterized by significant increases in total cholesterol and triglyceride levels and a marked reduction in high-density lipoprotein (HDL) concentrations compared with the normal control group ($p < 0.05$).

Table 5. Effects on serum lipid profile (% change vs. HFD).

Parameter	Semaglutide	Resveratrol	AIE-L	AIE-M	AIE-H
Total cholesterol	−32%	−31%	−33%	−34%	−33%
Triglycerides	−38%	−25%	−29%	−35%	−41%
HDL	+38%	+44%	+46%	+47%	+64%

Notes: Values in the main text table represent percentage changes relative to the HFD control group. Longitudinal serum lipid concentration data (mean ± SD, mg/dL) for total cholesterol, triglycerides, and HDL-C across all experimental timepoints are detailed in Supplementary Table S3.

During the treatment phase, the HFD control group exhibited further deterioration of lipid parameters, indicating progressive metabolic impairment. In contrast, treatment with semaglutide and resveratrol significantly improved lipid profiles compared with the HFD control ($p < 0.05$), demonstrating their lipid-lowering effects.

Administration of *A. integer* extract resulted in a dose-dependent improvement in serum lipid parameters. The highest dose (800 mg/kg) markedly reduced total cholesterol and triglyceride levels while significantly increasing HDL concentrations ($p < 0.05$ vs. HFD), with effects comparable to semaglutide. The intermediate (400 mg/kg) and low (200 mg/kg) doses also improved lipid profiles, although to a lesser extent.

Notably, the improvement in lipid parameters was consistent with the observed modulation of adipokines and body weight reduction, suggesting coordinated regulation of systemic lipid metabolism. The consistent improvement across all lipid parameters indicates a coordinated systemic effect rather than isolated metabolic changes. Percentage modifications in serum lipid parameters relative to the HFD control group are presented in Table 5. Corresponding longitudinal absolute concentration values (mean ± SD) for total cholesterol (mg/dL), triglycerides (mg/dL), and HDL-C (mg/dL) across all three experimental timepoints (before HFD, after HFD, and after treatment) are detailed in Supplementary Table S3.

3.6. Molecular Mechanisms Underlying the Anti-Obesity Effects of A. integer Extract

3.6.1. Modulation of Lipid Metabolism-Related Gene Expression

The relative mRNA expression levels of genes involved in lipid metabolism are presented in Table 6. High-fat diet (HFD) feeding markedly disrupted metabolic gene regulation, as evidenced by significant upregulation of the lipogenic genes *Fas* and *Pparγ* ($p < 0.05$ vs. normal), indicating enhanced lipogenesis and adipogenesis. In parallel, expression of *Cpt-1*, a key regulator of mitochondrial fatty acid β-oxidation, was not detected, suggesting impaired lipid catabolism. Expression of *AdipoR1* was moderately increased, likely reflecting compensatory alterations in adiponectin signaling.

Table 6. Effects on lipid metabolism-related gene expression (% change vs. HFD).

Gene	Semaglutide	Resveratrol	AIE-H
Fas	+36%	−85%	−74%
Pparγ	−25%	−84%	−68%
Cpt-1	n.d → ↑	+49%	n.d. → ↑
AdipoR1	−61%	−36%	−42%

Notes: Values in the main text table represent percentage changes relative to the HFD control group; n.d., not detected. Quantitative relative mRNA expression levels ($2^{-\Delta\Delta C_T}$, mean ± SD) for Fas, Cpt-1, Pparg, and Adipor1 across all treatment cohorts are provided in Supplementary Table S4.

Treatment with semaglutide significantly upregulated *Cpt-1* expression ($p < 0.05$ vs. HFD), indicating activation of fatty acid oxidation pathways, although lipogenic gene expression remained elevated. Resveratrol markedly suppressed *Fas* and *Pparγ* expression and strongly increased *Cpt-1*, consistent with its established role in promoting β-oxidation.

Administration of *A. integer* extract significantly modulated lipid metabolism-related gene expression in a manner consistent with a shift from lipid storage toward lipid utilization. The highest dose (800 mg/kg) significantly downregulated *Fas* and *Pparγ* while partially restoring *Cpt-1* expression ($p < 0.05$ vs. HFD). In addition, *AdipoR1* expression was normalized toward control levels, in agreement with the observed restoration of circulating adiponectin.

Relative percentage differences in adipose tissue gene expression compared to the HFD control group are summarized in Table 6. Absolute relative fold-change values ($2^{-\Delta\Delta C_T}$, mean ± SD) for *Fas*, *Cpt-1*, *Pparg*, and *Adipor1* across all treatment groups are compiled in Supplementary Table S4.

Taken together, these findings suggest that *A. integer* extract suppresses lipogenesis and adipogenesis while partially reactivating fatty acid oxidation pathways, supporting its role as a metabolic modulator targeting peripheral lipid homeostasis.

3.6.2. Modulation of Hypothalamic Appetite-Regulating Gene Expression

The relative mRNA expression levels of hypothalamic appetite-regulating genes are presented in Table 7. HFD feeding induced profound dysregulation of central appetite signaling, characterized by marked upregulation of the orexigenic gene *Npy* and downregulation of the anorexigenic genes *Pomc* and *Mc4r* ($p < 0.05$ vs. normal), indicating enhanced hunger signaling and impaired satiety control.

Table 7. Effects of *A. integer* extract on hypothalamic appetite-regulating gene expression (% change vs. HFD).

Gene	Semaglutide	Resveratrol	AIE-H
Pomc	+145.8%	−30.6%	+163.9%
Npy	−40.6%	−15.9%	−33.8%
Mc4r	+108.8%	−29.8%	+184.2%

Notes: Values in the main text table represent percentage changes relative to the HFD control group. Quantitative hypothalamic mRNA expression levels ($2^{-\Delta\Delta C_T}$, mean ± SD) for Pomc, Npy, and Mc4r across treatment cohorts are reported in Supplementary Table S5.

Semaglutide treatment significantly restored anorexigenic signaling, as evidenced by increased *Pomc* and *Mc4r* expression and reduced *Npy* levels ($p < 0.05$ vs. HFD). In contrast, resveratrol exerted limited effects on central pathways, with partial suppression of *Npy* but minimal recovery of *Pomc* and *Mc4r* expression.

Administration of *A. integer* extract markedly improved hypothalamic gene expression profiles. The highest dose (800 mg/kg) significantly upregulated *Pomc* and *Mc4r* while

suppressing *Npy* expression ($p < 0.05$ vs. HFD), indicating restoration of anorexigenic signaling and inhibition of orexigenic drive.

Relative percentage changes in hypothalamic mRNA expression compared to HFD controls are reported in Table 7. Quantitative fold-change levels ($2^{-\Delta\Delta C_T}$, mean ± SD) for *Pomc*, *Npy*, and *Mc4r* across treatment cohorts are provided in Supplementary Table S5.

These results demonstrate that *A. integer* extract effectively rebalances hypothalamic appetite regulation, consistent with its observed anorexigenic effects on food intake. Interestingly, the coordinated modulation of both anorexigenic and orexigenic pathways suggests a balanced regulatory effect on hypothalamic signaling.

3.6.3. Integrated Mechanistic Interpretation

Taken together, *A. integer* extract exerts anti-obesity effects through coordinated modulation of both peripheral and central regulatory pathways. Peripherally, the extract suppresses lipogenesis and adipogenesis while partially restoring fatty acid oxidation, thereby improving lipid utilization. Centrally, it restores hypothalamic appetite signaling by activating the *POMC–MC4R* axis and suppressing *Npy*-mediated orexigenic pathways.

This dual mechanism highlights a multi-target pharmacological profile, distinguishing *A. integer* extract from single-target agents and supporting its potential as a phytotherapeutic candidate for obesity management.

3.7. Effects of A. integer Extract on Adipocyte Morphology and Histopathology

Morphometric analysis of adipose tissue is summarized in Table 8, and representative histological images are shown in Figure 2. High-fat diet (HFD) feeding resulted in significant adipocyte hypertrophy, as evidenced by increased cell diameter and circumference compared with the normal control group ($p < 0.05$), indicating excessive lipid accumulation within adipocytes.

Table 8. Effects of *A. integer* extract on adipocyte size (% change vs. HFD).

Parameter	Semaglutide	Resveratrol	AIE-L	AIE-M	AIE-H
Adipocyte circumference	−27.1%	−16.2%	−9.4%	−26.0%	−18.3%
Adipocyte diameter	−27.2%	−16.2%	−9.4%	−26.0%	−18.3%

Notes: Values in the main text table represent percentage changes relative to the HFD control group. Absolute morphometric values (mean ± SD) for adipocyte circumference (μm) and diameter (μm) across all individual treatment groups are provided in Supplementary Table S6.

Treatment with semaglutide and resveratrol significantly reduced adipocyte size ($p < 0.05$ vs. HFD), consistent with decreased lipid storage. Similarly, administration of *A. integer* extracts attenuated adipocyte hypertrophy in a dose-dependent manner. The highest dose (800 mg/kg) significantly reduced adipocyte diameter and circumference ($p < 0.05$ vs. HFD), with values approaching those observed in the semaglutide-treated group. The intermediate and low doses also improved morphometric parameters, although to a lesser extent.

Histopathological evaluation corroborated the morphometric findings. Adipose tissue from the HFD group exhibited enlarged, hypertrophic adipocytes with disrupted tissue architecture, whereas extract-treated groups displayed smaller adipocytes and improved structural organization. Notably, the highest dose of *A. integer* extract restored adipose tissue morphology to a pattern comparable to that of the normal control.

Percentage reductions in epididymal adipocyte dimensions relative to the HFD control group are presented in Table 8. Absolute histological morphometric measurements (mean ± SD), including adipocyte circumference (μm) and diameter (μm), across all indi-

vidual treatment cohorts are compiled in Supplementary Table S6. These results demonstrate that *A. integer* extract effectively mitigates adipocyte hypertrophy and improves adipose tissue architecture, supporting its role in reducing lipid accumulation and modulating adipose tissue remodeling in obesity.

4. Discussion

Notably, the observed effects appear to arise from a coordinated multi-target mechanism, which may offer an advantage over single-target pharmacological approaches. The present study demonstrates that the ethanol extract of *Artocarpus integer* stem bark exerts significant anti-obesity effects in a high-fat diet (HFD)-induced obese rat model through coordinated modulation of central appetite regulation and peripheral lipid metabolism. The extract attenuated body weight gain, reduced visceral adiposity, improved lipid profiles, restored adipokine balance, and ameliorated adipocyte hypertrophy, indicating broad metabolic efficacy [19].

HFD feeding successfully induced a pathological obese phenotype, characterized by increased body weight, adipose tissue expansion, dyslipidemia, and disruption of endocrine and neuroregulatory pathways [20]. Elevated leptin levels observed in the HFD group are consistent with leptin resistance, a hallmark of obesity associated with impaired hypothalamic signaling despite hyperleptinemia [21]. Concurrent increases in amylin and reductions in adiponectin further reflect metabolic dysregulation and impaired adipose tissue function [22]. These findings align with previous reports demonstrating that obesity is associated with altered adipokine profiles and disrupted energy homeostasis [23]. The relatively high doses used in this preclinical study are typical for crude plant extracts; dose optimization and pharmacokinetic studies are required to determine clinically relevant exposure levels [24]. In addition, while the current panel demonstrated clear improvements in total cholesterol, triglycerides, and HDL, direct quantification of circulating free fatty acids (FFAs) and LDL subfractions was not included due to volume constraints. Future detailed lipidomic investigations will be essential to fully map the extract's impact on peripheral lipolysis rates and lipoprotein clearance [25,26].

Treatment with *A. integer* extract significantly reduced body weight gain and visceral adiposity in a dose-dependent manner, with the highest dose demonstrating robust weight-lowering activity relative to semaglutide. This effect was accompanied by reduced food intake, suggesting a central anorexigenic mechanism. At the molecular level, the extract restored hypothalamic signaling by upregulating *Pomc* and *Mc4r* and suppressing *Npy*, indicating activation of the *Pomc–Mc4r* axis and inhibition of orexigenic pathways [27]. This pattern closely resembles the mechanism of action of GLP-1 receptor agonists, which enhance satiety signaling and suppress appetite through hypothalamic pathways [28]. Notably, compared with resveratrol, which showed limited effects on central gene expression, *A. integer* extract demonstrated a more balanced regulation of both anorexigenic and orexigenic pathways, highlighting its potential advantage as a multi-target agent.

We also added an explicit statement in the Discussion section limitations acknowledging that formal non-inferiority or equivalence testing was not performed and that direct comparative efficacy claims cannot be drawn without dedicated trial designs. In addition to central effects, *A. integer* extracts significantly modulated peripheral lipid metabolism. Downregulation of *Fas* and *Pparγ* indicates suppression of lipogenesis and adipogenesis [29], while partial restoration of *Cpt-1* expression suggests reactivation of mitochondrial fatty acid β-oxidation [30]. The absence of detectable Cpt-1 expression in the HFD group primarily reflects severe transcriptional suppression of mitochondrial β-oxidation under obesogenic conditions [31], supported by preserved reference gene (β-actin) integrity across all samples; however, technical factors related to the lower limit of qPCR detection may

also contribute and are acknowledged. Normalization of *AdipoR1* expression, together with increased circulating adiponectin, further supports improved adiponectin signaling and metabolic homeostasis [32]. These molecular changes are consistent with the observed improvements in serum lipid profile and adipose tissue morphology, indicating a shift from lipid storage toward enhanced lipid utilization.

The observed modulation of lipid metabolism-related gene expression suggests the involvement of upstream energy-sensing pathways [33]. In particular, the coordinated downregulation of *Fas* and *Pparγ* and partial restoration of *Cpt-1* expression may be indicative of activation of AMP-activated protein kinase (AMPK), a central regulator of cellular energy homeostasis that inhibits lipogenesis and promotes fatty acid β-oxidation [34]. This putative AMPK-mediated mechanism is further supported by the presence of stilbene and chalcone derivatives identified in the extract, which have been reported to activate AMPK signaling in metabolic tissues [35,36]. Although AMPK activation was not directly assessed in the present study, these findings suggest that *A. integer* extract may exert its anti-obesity effects, at least in part, through AMPK-dependent pathways. However, direct assessment of AMPK phosphorylation would be required to confirm this mechanism.

Furthermore, while RT–qPCR provided clear evidence of transcriptional modulation across central and peripheral targets, protein-level validation via Western blot was not performed due to tissue volume constraints during multi-parameter testing. Although functional outcomes (food intake, adipokine concentrations, lipid profiles, and adipocyte histology) strongly align with the observed gene expression patterns, direct evaluation of protein abundance and post-translational modifications remains an essential objective for future mechanistic studies [37].

Crucially, comparing Cpt-1 expression profiles across treatments reveals distinct upstream mechanisms converging on a shared metabolic outcome. Resveratrol produced a direct, robust upregulation of Cpt-1 (+49%), reflecting its primary action as a peripheral activator of mitochondrial β-oxidation via SIRT1/AMPK pathways. In contrast, semaglutide reactivated Cpt-1 transcription (n.d. $\rightarrow \uparrow$) secondarily by suppressing food intake and relieving nutrient excess. *A. integer* extract (800 mg/kg) uniquely combines both modes: direct peripheral stimulation by bioactive polyphenols alongside caloric-restriction-mediated derepression. These distinct regulatory pathways explain how different molecular drivers achieve comparable reductions in circulating triglycerides and adipocyte hypertrophy.

The improvement in adipocyte morphology provides additional structural evidence supporting the metabolic effects of the extract [38]. Reduction in adipocyte size and restoration of tissue architecture indicate decreased lipid accumulation and improved adipose tissue remodeling [39]. Given that adipocyte hypertrophy is closely linked to insulin resistance and chronic inflammation [40], attenuation of adipocyte enlargement may contribute to the overall metabolic benefits observed in this study [41].

Phytochemical profiling by LC–HRMS revealed the presence of stilbene derivatives, chalcones, prenylated flavonoids, and triterpenoids, which are known to exert anti-obesity effects through multiple mechanisms [42,43]. Stilbenes, such as resveratrol, are associated with activation of AMPK/SIRT1 signaling and enhancement of fatty acid oxidation [44], whereas chalcones and flavonoids have been reported to inhibit adipogenesis and suppress lipogenic gene expression [45]. The coexistence of these bioactive compounds suggests potential synergistic interactions, enabling simultaneous modulation of central and peripheral pathways [46]. Such multi-component, multi-target activity represents a key advantage over single-compound therapies and aligns with current pharmacological strategies for complex metabolic disorders [47]. The contribution of individual compounds remains to be elucidated through bioactivity-guided fractionation [48].

Natural chalcones (such as xanthohumol and related prenylated derivatives) directly inhibit de novo lipogenesis (DNL) and enhance fatty acid oxidation by targeting the LKB1/SIRT1–AMPK axis, thereby downregulating SREBP-1c and acetyl-CoA carboxylase (ACC) while upregulating CPT1 and hormone-sensitive lipase (HSL) [49]. Polyphenolic secondary metabolites mitigate lipid accumulation by remodeling the plasma lipidome, suppressing early differentiation signals in preadipocytes, and downregulating downstream lipogenic targets such as fatty acid synthase (FASN) and FABP4 [50]. Although AMPK activation was not directly measured, the observed gene expression profile is consistent with this pathway and warrants further investigation.

Importantly, the dual action of *A. integer* extract distinguishes it from conventional therapies. While semaglutide primarily targets central appetite regulation [51] and resveratrol mainly influences peripheral metabolism [52], *A. integer* extract demonstrated integrated effects on both pathways. This coordinated mechanism may provide enhanced therapeutic efficacy, as effective obesity management requires simultaneous regulation of energy intake and metabolic processing [53].

Despite these promising findings, several limitations should be acknowledged. Compound identification was tentative and based on LC–HRMS analysis without structural confirmation. Further studies employing tandem mass spectrometry (MS/MS), compound isolation, and bioactivity-guided fractionation are required to identify the active constituents. In addition, long-term safety, pharmacokinetic profiling, and clinical validation are necessary to establish translational relevance.

Although no overt signs of toxicity were observed, dedicated toxicological studies are required to establish the safety profile. While these findings are promising, translation to human physiology requires careful validation in clinical studies.

5. Conclusions

The present study demonstrates that the 95% ethanol extract of *Artocarpus integer* stem bark exerts promising anti-obesity effects in a high-fat diet-induced obese rat model. The extract significantly attenuated body weight gain, reduced visceral adiposity, improved serum lipid profiles, restored adipokine balance, and mitigated adipocyte hypertrophy, indicating broad metabolic efficacy.

Mechanistically, these effects were associated with coordinated modulation of central and peripheral regulatory pathways, including activation of hypothalamic anorexigenic signaling (*Pomc* and *Mc4r*), suppression of the orexigenic gene (*Npy*), downregulation of lipogenic and adipogenic genes (*Fas* and *Pparγ*), and partial restoration of fatty acid oxidation via *Cpt-1*. This integrated mechanism supports a shift from energy storage toward energy utilization.

Phytochemical profiling revealed the presence of stilbene, chalcone, flavonoid, and triterpenoid derivatives, suggesting that the observed pharmacological effects may arise from synergistic multi-component interactions.

Overall, *A. integer* stem bark extract exhibits a multi-target pharmacological profile, highlighting its potential as a phytotherapeutic candidate for obesity management. Further studies are required to identify the active constituents, elucidate their precise molecular mechanisms, and evaluate long-term safety and translational applicability.

Supplementary Materials: The following supporting information can be downloaded at: https://www.mdpi.com/article/10.3390/applbiosci5030079/s1, Table S1: Comprehensive LC–HRMS profiling data, including retention times (RT), mass-to-charge ratios (m/z $[M+H]^+$), tentative compound identifications, and detailed annotations; Table S2: Effects of *A. integer* stem bark extract on food intake and appetite-related hormones; Table S3: Effects of *A. integer* stem bark extract on serum lipid profile in HFD-induced obese rats; Table S4: Effects of *A. integer* stem bark extract on lipid

metabolism-related gene expression in high-fat diet-induced obese rats; Table S5: Effects of *A. integer* stem bark extract on hypothalamic appetite-regulating gene expression in high-fat diet-induced obese rats; Table S6: Effects of *A. integer* stem bark extract on adipocyte size in HFD-induced obese rats.

Author Contributions: Conceptualization: A.B. and S.S.; Data curation: S.A.R. and A.R.; Formal analysis: A.B. and S.A.R.; Funding acquisition: A.B. and S.S.; Methodology: A.R., A.B. and S.S.; Investigation: S.A.R. and A.R.; Project administration: A.B.; Supervision: A.B. and S.S.; Validation: A.B.; Writing—original draft: A.B.; Writing—review and editing: A.B. and S.S. All authors have read and agreed to the published version of the manuscript.

Funding: This research was funded by the Indonesian Endowment Fund for Education (LPDP) on behalf of the Indonesian Ministry of Higher Education, Science and Technology, and managed under the EQUITY Program (Contract No. 4302/B3/DT.03.08/2025 and 573/PKS/R/UI/2025).

Institutional Review Board Statement: This study was approved by the Ethics Committee of the Faculty of Medicine, Universitas Indonesia—Cipto Mangunkusumo Hospital (Approval No. KET-72/UN2.F1/ETIK/PPM.00.02/2025, 10 January 2025).

Informed Consent Statement: Not applicable.

Data Availability Statement: The data supporting the findings of this study are available from the corresponding author upon reasonable request.

Acknowledgments: We thank the Laboratory of Pharmacology and Toxicology, Faculty of Pharmacy, Universitas Indonesia, for providing the facilities and technical support necessary for this study. We also appreciate the assistance of the student in the obesity research group, especially Ruth Putri Deva Chrisna, for the support during the experimental work. During the preparation of this manuscript, the authors used AI-assisted tools solely for language refinement and improvement of readability. All scientific content, data analysis, and interpretation were performed by the authors. The authors critically reviewed and edited the manuscript and take full responsibility for the accuracy and integrity of the work.

Conflicts of Interest: The authors declare no conflicts of interest.

Abbreviations

AIE	*Artocarpus integer* extract
AIE-L	*Artocarpus integer* extract (200 mg/kg)
AIE-M	*Artocarpus integer* extract (400 mg/kg)
AIE-H	*Artocarpus integer* extract (800 mg/kg)
HFD	High-fat diet
LC-HRMS	Liquid chromatography–high resolution mass spectrometry
mRNA	Messenger ribonucleic acid
SD	Standard deviation
TG	Triglycerides
HDL	High-density lipoprotein
BMI	Body mass index
BW	Body weight
Cpt-1	Carnitine palmitoyltransferase-1
Fas	Fatty acid synthase
GLP-1	Glucagon-like peptide-1
Mc4r	Melanocortin-4 receptor
Npy	Neuropeptide Y
Pomc	Proopiomelanocortin
Pparγ	Peroxisome proliferator-activated receptor gamma
AdipoR1	Adiponectin receptor 1

References

1. Młynarska, E.; Bojdo, K.; Bulicz, A.; Frankenstein, H.; Gąsior, M.; Kustosik, N.; Rysz, J.; Franczyk, B. Obesity as a Multifactorial Chronic Disease: Molecular Mechanisms, Systemic Impact, and Emerging Digital Interventions. *Curr. Issues Mol. Biol.* **2025**, *47*, 787. [CrossRef] [PubMed]
2. Kloock, S.; Ziegler, C.G.; Dischinger, U. Obesity and its comorbidities, current treatment options and future perspectives: Challenging bariatric surgery? *Pharmacol. Ther.* **2023**, *251*, 108549. [CrossRef] [PubMed]
3. Manoria, P.C. The Obesity Drug Revolution: New Frontiers in Pharmacotherapy. *Cureus* **2025**, *17*, e96713. [CrossRef] [PubMed]
4. Purcell, A.R.; Zhen, X.M.; Wong, J.; Glastras, S.J. Glucagon-like peptide-1 receptor agonist treatment reduces body weight and improves glycaemic outcomes in patients with concurrent overweight/obesity and type 1 diabetes: A systematic review and meta-analysis. *Diabetes Obes. Metab.* **2026**, *28*, 296–305. [CrossRef] [PubMed]
5. Park, J.S.; Kim, K.S.; Choi, H.J. Glucagon-Like Peptide-1 and Hypothalamic Regulation of Satiation: Cognitive and Neural Insights from Human and Animal Studies. *Diabetes Metab. J.* **2025**, *49*, 333–347. [CrossRef] [PubMed]
6. Benbaibeche, H.; Boumehira, A.Z.; Khan, N.A. Natural bioactive compounds and their mechanisms of action in the management of obesity: A narrative review. *Front. Nutr.* **2025**, *12*, 1614947. [CrossRef] [PubMed]
7. Kogut, Ł.; Puchalski, C.; Katryńska, D.; Zaguła, G. The Multidirectional Biological Activity of Resveratrol: Molecular Mechanisms, Systemic Effects and Therapeutic Potential—A Review. *Nutrients* **2026**, *18*, 313. [CrossRef] [PubMed]
8. Periferakis, A.-T.; Periferakis, A.; Troumpata, L.; Periferakis, K.; Scheau, A.-E.; Iftime, A.; Caruntu, A.; Badarau, I.A.; Caruntu, C.; Scheau, C. Biological Activity of Stilbenoids Against Fungal, Parasitic, and Viral Pathogens. *Molecules* **2026**, *31*, 830. [CrossRef] [PubMed]
9. Sari, A.K.; Rizki, M.I.; Azhara, D.D.; Fadlilaturrahmah, F. Antioxidant Activity and Marker Compound Levels of Cempedak Leaf (Artocarpus integer) Extract in Different Solvent Variations. *Trop. Health Med. Res.* **2024**, *6*, 36–44. [CrossRef]
10. Zeng, S.; Cao, J.; Wei, C.; Chen, Y.; Liu, Q.; Li, C.; Zhang, Y.; Zhu, K.; Wu, G.; Tan, L. Polysaccharides from Artocarpus heterophyllus Lam. (jackfruit) pulp alleviate obesity by modulating gut microbiota in high fat diet-induced rats. *Food Hydrocoll.* **2023**, *139*, 108521. [CrossRef]
11. Rendine, M.; Marino, M.; Martini, D.; Riso, P.; Møller, P.; Del Bo', C. Effect of (Poly)phenols on Lipid and Glucose Metabolisms in 3T3-L1 Adipocytes: An Integrated Analysis of Mechanistic Approaches. *Curr. Obes. Rep.* **2025**, *14*, 64. [CrossRef] [PubMed]
12. Bahtiar, A.; Musyantika, L.; Wahyuni, T.; Utami, R.A.; Siriamornpun, S. Edible Marine Red Alga Gracilaria coronopifolia as a Potential Functional Ingredient: Chemical Profiling and Metabolic Effects in Diet-Induced Obese Rats. *Foods* **2026**, *15*, 1167. [CrossRef] [PubMed]
13. Wardani, E.; Harahap, Y.; Mun'im, A.; Bahtiar, A. Evaluation of the combination of Kemuning Leaves Extracts and Simvastatin on Blood fatty acids and amino acids of Hyperlipidemic Model Rats. *Res. J. Pharm. Technol.* **2021**, *14*, 2076–2080. [CrossRef]
14. Dwitiyanti, D.; Harahap, Y.; Elya, B.; Bahtiar, A. Binahong (Anredera cordifolia (Tenore) Steen.) Leaf Extract Modulates Fatty Acids and Amino Acids to Lower Blood Glucose in High-Fat Diet-Induced Diabetes Mellitus Rats. *Adv. Pharmacol. Pharm. Sci.* **2021**, *2021*, 8869571. [CrossRef] [PubMed]
15. Haneishi, Y.; Noguchi, T.; Furusho, T.; Yamauchi, J.; Tanioka, Y. Characterization of Breadfruit (Artocarpus altilis) and Its Long-Term Effect on Glucose and Lipid Metabolism in Rats Fed with a High-Fat Diet. *ACS Food Sci. Technol.* **2025**, *5*, 3544–3553. [CrossRef]
16. Cawthon, C.R.; Blonde, G.D.; Nisi, A.V.; Bloomston, H.M.; Krubitski, B.; le Roux, C.W.; Spector, A.C. Chronic Semaglutide Treatment in Rats Leads to Daily Excessive Concentration-Dependent Sucrose Intake. *J. Endocr. Soc.* **2023**, *7*, bvad074. [CrossRef] [PubMed]
17. de Silva, A.; Bloom, S.R. Gut Hormones and Appetite Control: A Focus on PYY and GLP-1 as Therapeutic Targets in Obesity. *Gut Liver* **2012**, *6*, 10–20. [CrossRef] [PubMed]
18. Slaoui, M.; Fiette, L. *Histopathology Procedures: From Tissue Sampling to Histopathological Evaluation*; Springer: Berlin/Heidelberg, Germany, 2011; pp. 69–82. [CrossRef] [PubMed]
19. Gudasi, S.; Patil, M.B. Comprehensive review on anti-obesity effects of plant-derived compounds: Evidence from 3T3-L1 adipocytes and high-fat diet models. *Asp. Mol. Med.* **2025**, *5*, 100089. [CrossRef]
20. Sun, S.; Zhang, H.; Chen, J.; Hei, K.; Hou, Y.; Yang, Y.; Shan, C.; Zhang, L. High-fat diet-induced dyslipidemia drives retinal ECE-1 and ET-1 upregulation. *Front. Endocrinol.* **2025**, *16*, 1640890. [CrossRef] [PubMed]
21. Hu, W.; Zhu, H.; Gong, F. Leptin and leptin resistance in obesity: Current evidence, mechanisms and future directions. *Endocr. Connect.* **2025**, *14*, e250521. [CrossRef] [PubMed]
22. Jouy, S.H.; Mohan, S.; Scichilone, G.; Mostafa, A.; Mahmoud, A.M. Adipokines in the Crosstalk between Adipose Tissues and Other Organs: Implications in Cardiometabolic Diseases. *Biomedicines* **2024**, *12*, 2129. [CrossRef] [PubMed]
23. Clemente-Suárez, V.J.; Redondo-Flórez, L.; Beltrán-Velasco, A.I.; Martín-Rodríguez, A.; Martínez-Guardado, I.; Navarro-Jiménez, E.; Laborde-Cárdenas, C.C.; Tornero-Aguilera, J.F. The Role of Adipokines in Health and Disease. *Biomedicines* **2023**, *11*, 1290. [CrossRef] [PubMed]

24. Jia, Q.; He, Q.; Yao, L.; Li, M.; Lin, J.; Tang, Z.; Zhu, X.; Xiang, X. Utilization of Physiologically Based Pharmacokinetic Modeling in Pharmacokinetic Study of Natural Medicine: An Overview. *Molecules* **2022**, *27*, 8670. [CrossRef] [PubMed]
25. Géhin, C.; Fowler, S.J.; Trivedi, D.K. Chewing the fat: How lipidomics is changing our understanding of human health and disease in 2022. *Anal. Sci. Adv.* **2023**, *4*, 104–131. [CrossRef] [PubMed]
26. Xu, J.; Lu, D.; Huang, X. Lipid metabolism and metabolites: Emerging roles in systemic physiology and metabolic diseases. *J. Genet. Genom.* **2026**, *53*, 1143–1158. [CrossRef] [PubMed]
27. Martins, F.F.; Santos-Reis, T.; Marinho, T.S.; Aguila, M.B.; Mandarim-de-Lacerda, C.A. Hypothalamic anorexigenic signaling pathways (leptin, amylin, and proopiomelanocortin) are semaglutide (GLP-1 analog) targets in obesity control in mice. *Life Sci.* **2023**, *313*, 121268. [CrossRef] [PubMed]
28. Moiz, A.; Filion, K.B.; Tsoukas, M.A.; Yu, O.H.Y.; Peters, T.M.; Eisenberg, M.J. Mechanisms of GLP-1 Receptor Agonist-Induced Weight Loss: A Review of Central and Peripheral Pathways in Appetite and Energy Regulation. *Am. J. Med.* **2025**, *138*, 934–940. [CrossRef] [PubMed]
29. Nematbakhsh, S.; Pei, C.P.; Selamat, J.; Nordin, N.; Idris, L.H.; Razis, A.F.A. Molecular Regulation of Lipogenesis, Adipogenesis and Fat Deposition in Chicken. *Genes* **2021**, *12*, 414. [CrossRef] [PubMed]
30. Sebastián, D.; Guitart, M.; García-Martínez, C.; Mauvezin, C.; Orellana-Gavaldà, J.M.; Serra, D.; Gómez-Foix, A.M.; Hegardt, F.G.; Asins, G. Novel role of FATP1 in mitochondrial fatty acid oxidation in skeletal muscle cells. *J. Lipid Res.* **2009**, *50*, 1789–1799. [CrossRef] [PubMed]
31. Yang, W.; Pang, N.; He, X. Breaking the metabolic–inflammatory vicious cycle in polycystic ovary syndrome: A comparative review of ketogenic and high-fat diets. *Lipids Health Dis.* **2025**, *24*, 310. [CrossRef] [PubMed]
32. Wang, Q.; Wang, X.; Xu, D.; Jiang, M.; Gao, Y.; Jiang, L.; Liu, M.; Tang, H.; Tang, L. Circulating levels of adiponectin and AdipoR expression in peripheral blood mononuclear cells are associated with lower respiratory tract Infection. *Front. Immunol.* **2025**, *15*, 1510760. [CrossRef] [PubMed]
33. Khan, F.; Elsori, D.; Verma, M.; Pandey, S.; Rab, S.O.; Siddiqui, S.; Alabdallah, N.M.; Saeed, M.; Pandey, P. Unraveling the intricate relationship between lipid metabolism and oncogenic signaling pathways. *Front. Cell Dev. Biol.* **2024**, *12*, 1399065. [CrossRef] [PubMed]
34. Liu, H.; Wang, S.; Wang, J.; Guo, X.; Song, Y.; Fu, K.; Gao, Z.; Liu, D.; He, W.; Yang, L.-L. Energy metabolism in health and diseases. *Signal Transduct. Target. Ther.* **2025**, *10*, 69. [CrossRef] [PubMed]
35. Kaewin, S.; Poolsri, W.; Korkut, G.G.; Patrakka, J.; Aiebchun, T.; Rungrotmongkol, T.; Sungkaworn, T.; Sukanadi, I.; Chavasiri, W.; Muanprasat, C. A sulfonamide chalcone AMPK activator ameliorates hyperglycemia and diabetic nephropathy in db/db mice. *Biomed. Pharmacother.* **2023**, *165*, 115158. [CrossRef] [PubMed]
36. Brás, L.P.; Luís, Â.; Chatel, G.; Socorro, S.; Duarte, A.P. Stilbenes from Vine Extracts: Therapeutic Potential and Mechanisms. *Int. J. Mol. Sci.* **2025**, *26*, 8269. [CrossRef] [PubMed]
37. Kurhaluk, N.; Kołodziejska, R.; Mazur, Z.; Lukash, O.; Yakovenko, O.; Tkaczenko, H. Functional Foods as Modulators of Epigenetic Mechanisms Affecting Metabolic Health in Adolescence. *Int. J. Mol. Sci.* **2026**, *27*, 2066. [CrossRef] [PubMed]
38. Pincu, Y.; Yoel, U.; Haim, Y.; Makarenkov, N.; Maixner, N.; Shaco-Levy, R.; Bashan, N.; Dicker, D.; Rudich, A. Assessing Obesity-Related Adipose Tissue Disease (OrAD) to Improve Precision Medicine for Patients Living With Obesity. *Front. Endocrinol.* **2022**, *13*, 860799. [CrossRef] [PubMed]
39. Abuhattum, S.; Kotzbeck, P.; Schlüßler, R.; Harger, A.; de Schellenberger, A.A.; Kim, K.; Escolano, J.-C.; Müller, T.; Braun, J.; Wabitsch, M.; et al. Adipose cells and tissues soften with lipid accumulation while in diabetes adipose tissue stiffens. *Sci. Rep.* **2022**, *12*, 10325. [CrossRef] [PubMed]
40. Choo, Y.N.; Ravi, R.N.; Subramaniyan, V. Insulin resistance induced by obesity: Mechanisms, metabolic implications and therapeutic approaches. *Mol. Biol. Rep.* **2026**, *53*, 357. [CrossRef] [PubMed]
41. White, U. Adipose tissue expansion in obesity, health, and disease. *Front. Cell Dev. Biol.* **2023**, *11*, 1–4. [CrossRef] [PubMed]
42. Scarpa, E.-S.; Amatori, S.; Caprioli, G.; Maggi, F.; Moroncini, G.; Balercia, G.; Giacchetti, G. Innovative Therapeutic Approaches Targeting Obesity: Can Flavonoids Improve the Efficacy of Anti-Obesogenic Drugs? *Int. J. Mol. Sci.* **2025**, *26*, 10142. [CrossRef] [PubMed]
43. Lv, H.-W.; Wang, Q.-L.; Luo, M.; Zhu, M.-D.; Liang, H.-M.; Li, W.-J.; Cai, H.; Zhou, Z.-B.; Wang, H.; Tong, S.-Q.; et al. Phytochemistry and pharmacology of natural prenylated flavonoids. *Arch. Pharm. Res.* **2023**, *46*, 207–272. [CrossRef] [PubMed]
44. Akinwumi, B.; Bordun, K.-A.; Anderson, H. Biological Activities of Stilbenoids. *Int. J. Mol. Sci.* **2018**, *19*, 792. [CrossRef] [PubMed]
45. Maisto, M.; Marzocchi, A.; Keivani, N.; Piccolo, V.; Summa, V.; Tenore, G.C. Natural Chalcones for the Management of Obesity Disease. *Int. J. Mol. Sci.* **2023**, *24*, 15929. [CrossRef] [PubMed]
46. Aydemir, E.; Şimşek, B.; Acar, A.; Kilit, A.C.; Köse, E.O. Therapeutic Potential of Kuwanon G: From Bioactivities to Network-Level Mechanisms. *Molecules* **2026**, *31*, 2292. [CrossRef] [PubMed]
47. Lempesis, I.G.; Dalamaga, M. Obesity pharmacotherapy reimagined: The era of multi-receptor agonists and next-generation metabolic modulators, perspectives and controversies. *Metabol. Open* **2026**, *30*, 100463. [CrossRef] [PubMed]

48. Mani, J.; Johnson, J.; Hosking, H.; Hoyos, B.E.; Walsh, K.B.; Neilsen, P.; Naiker, M. Bioassay Guided Fractionation Protocol for Determining Novel Active Compounds in Selected Australian Flora. *Plants* **2022**, *11*, 2886. [CrossRef] [PubMed]
49. Adhikari, S.; Nath, P.; Deb, V.K.; Das, N.; Banerjee, A.; Pathak, S.; Duttaroy, A.K. Pharmacological potential of natural chalcones: A recent studies and future perspective. *Front. Pharmacol.* **2025**, *16*, 1570385. [CrossRef] [PubMed]
50. Wei, H.; Rui, J.; Yan, X.; Xu, R.; Chen, S.; Zhang, B.; Wang, L.; Zhang, Z.; Zhu, C.; Ma, M.; et al. Plant polyphenols as natural bioactives for alleviating lipid metabolism disorder: Mechanisms and application challenges. *Food Res. Int.* **2025**, *203*, 115682. [CrossRef] [PubMed]
51. Papakonstantinou, I.; Tsioufis, K.; Katsi, V. Spotlight on the Mechanism of Action of Semaglutide. *Curr. Issues Mol. Biol.* **2024**, *46*, 14514–14541. [CrossRef] [PubMed]
52. Bitterman, J.L.; Chung, J.H. Metabolic effects of resveratrol: Addressing the controversies. *Cell. Mol. Life Sci.* **2015**, *72*, 1473–1488. [CrossRef] [PubMed]
53. Żurawski, T.; Bartosiewicz, A. Dietary and Behavioral Strategies for Weight Loss and Weight Loss Maintenance: A Narrative Review. *Nutrients* **2025**, *18*, 12. [CrossRef] [PubMed]

Disclaimer/Publisher's Note: The statements, opinions and data contained in all publications are solely those of the individual author(s) and contributor(s) and not of MDPI and/or the editor(s). MDPI and/or the editor(s) disclaim responsibility for any injury to people or property resulting from any ideas, methods, instructions or products referred to in the content.